

Quantifying Residual Stress in Nanoscale Thin Polymer Films *via* Surface Wrinkling

Jun Young Chung, Thomas Q. Chastek, Michael J. Fasolka, Hyun Wook Ro, and Christopher M. Stafford*

Polymers Division, National Institute of Standards and Technology, 100 Bureau Drive, Gaithersburg, Maryland 20899

ABSTRACT Residual stress, a pervasive consequence of solid materials processing, is stress that remains in a material after external forces have been removed. In polymeric materials, residual stress results from processes, such as film formation, that force and then trap polymer chains into nonequilibrium stressed conformations. In solvent-cast films, which are central to a wide range of technologies, residual stress can cause detrimental effects, including microscopic defect formation and macroscopic dimensional changes. Since residual stress is difficult to measure accurately, particularly in nanoscale thin polymer films, it remains a challenge to understand and control. We present here a quantitative method of assessing residual stress in polymer thin films by monitoring the onset of strain-induced wrinkling instabilities. Using this approach, we show that thin (> 100 nm) polystyrene films prepared *via* spin-coating possess residual stresses of ≈ 30 MPa, close to the crazing and yield stress. In contrast to conventional stress measurement techniques such as wafer curvature, our technique has the resolution to measure residual stress in films as thin as 25 nm. Furthermore, we measure the dissipation of residual stress through two relaxation mechanisms: thermal annealing and plasticizer addition. In quantifying the amount of residual stress in these films, we find that the residual stress gradually decreases with increasing annealing time and plasticizer amounts. Our robust and simple route to measure residual stress adds a key component to the understanding of polymer thin film behavior and will enable identification of more effective processing routes that mitigate the detrimental effects of residual stress.

KEYWORDS: coatings · mechanical properties · nanoscale thin films · polymers · residual stress · small-angle light scattering · surface wrinkling

When materials are processed into useful structures or devices, they are often trapped in a nonequilibrium state. One important mechanical manifestation of molecular scale nonequilibrium is residual stress.¹ Left unchecked, residual stress can severely reduce materials' performance and reliability by inducing mechanical instabilities, such as warpage and buckle-delamination, or it can increase the probability of defect formation or complete interfacial failure.² For polymers, residual stress is related to the macromolecules locking into nonequilibrium configurations during fast processes, such as solvent casting.^{2–6} Residual stress can also lead to the destabilization of polymer films, such as dewetting processes.^{7–10} Thin film coatings and nanoscale devices

of polymer materials exacerbate this concern since these technologies are intolerant to the failures and defects that residual stress can produce. As there are many factors, such as processing routes, thermal history, and polymer characteristics (*e.g.*, molecular weight, glass transition temperature, and elastic stiffness), that contribute to this phenomenon, the understanding and control of residual stress in polymer thin films remains a challenge.²

There are many methods available to measure residual stress in polymer films, including curvature or deflection-based,^{3–5,11,12} membrane bulge,¹³ blister,¹⁴ cylindrical punch,¹⁵ and fluorescence methods.^{16,17} The curvature or deflection of a thin film coated substrate is among the most commonly used. This technique relates the deflection of a thick elastic substrate (*e.g.*, silicon wafer or cantilever arm) to the average residual stress of the thin film.^{18,19} Though the measurement is straightforward, this technique is limited by its sensitivity for resolving small changes in curvature.²⁰ Hence, this technique becomes markedly less reliable as films become increasingly thin and deformations become very small. The sensitivity can be enhanced when applied to thinner substrates; however, wafers with a thickness below 100 μm are fragile and require special handling.²⁰ Therefore, there is a measurement need for accurately quantifying residual stress in polymer thin films. Additionally, this metrology can improve the understanding and control of residual stress in order to optimize the performance of polymer coatings used in numerous nanoscale device applications such as next-generation lithography, organic electronics, and sensors. To address

*Address correspondence to chris.stafford@nist.gov.

Received for review December 12, 2008 and accepted March 03, 2009.

Published online March 19, 2009.
10.1021/nn800853y CCC: \$40.75

© 2009 American Chemical Society

this challenge, we present a new method based on a surface wrinkling phenomenon^{21–35} to accurately quantify the residual stresses in nanoscale thin polymer films.

Surface wrinkling can occur in systems comprised of an elastic film adhered to a relatively thick, compliant elastic substrate. Compression of this composite above the critical strain (ϵ_c) produces a periodic wrinkling pattern; the dimensions and onset of wrinkle formation are related to the mechanical properties of the polymer film.²¹ For small strains, the equilibrium wavelength (λ) of the wrinkling pattern can be described as^{22–25}

$$\lambda = 2\pi h_f \left(\frac{\bar{E}_f}{3\bar{E}_s} \right)^{1/3} \quad (1)$$

where h is the thickness and $\bar{E} = E/(1 - \nu^2)$ is the plane-strain modulus (E is the elastic modulus, ν is the Poisson's ratio, and the subscripts f and s denote the film and substrate, respectively). The amplitude of wrinkle pattern (A) increases with a square-root dependence on the compressive strain (ϵ) as

$$A = h_f \left(\frac{\epsilon}{\epsilon_c} - 1 \right)^{1/2} \quad (2)$$

Several mechanics models have been developed for predicting an expected "critical strain", defined as the minimum strain needed to induce wrinkling.^{22–26} The theoretical critical strain (ϵ_{c0}) solution for the uniaxial strain state, shown in eq 3 (ref 36), is among the most widely known.^{24–29}

$$\epsilon_{c0} = \frac{1}{4} \left(\frac{3\bar{E}_s}{\bar{E}_f} \right)^{2/3} \quad (3)$$

In this work, we have selected materials whose properties can be measured accurately within the range of small strains. Therefore, we are able to utilize the above wrinkling relationships, which are based on linear elasticity without additional assumptions, to accurately measure the properties of our materials.

A primary advantage of using surface wrinkling as a metrology for thin film properties lies in the ability to optically observe the wrinkle patterns; hence, this avoids common limitations in sensitivity.³³ For example, a 25 nm thick polymer film can have a wrinkling wavelength $> 1 \mu\text{m}$. The application of surface wrinkling to quantitatively relate the wrinkling wave-

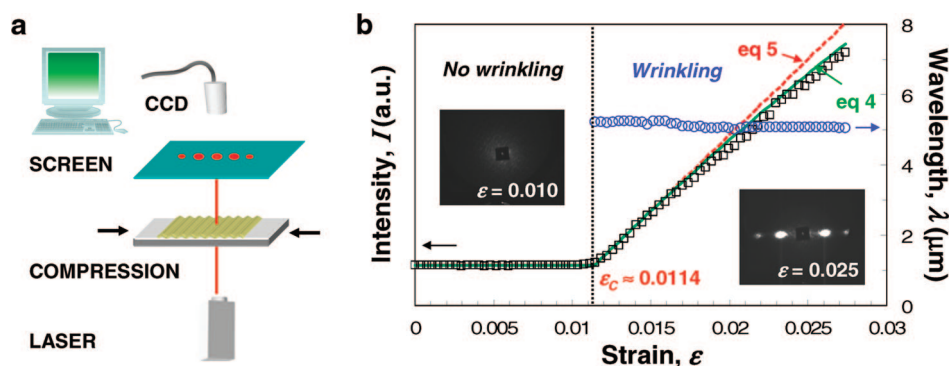


Figure 1. (a) Schematic of the custom-built SALS apparatus. The diffraction pattern from the wrinkled film is projected onto a screen and acquired by CCD camera. (b) Representative plot depicting first-order diffraction intensity (open squares) versus compressive strain. The insets show the representative SALS diffraction patterns observed below and above the critical strain for the onset of wrinkling (ϵ_c). The dominant wavenumber (q_0) is measured from the location of the first diffraction peaks, and the wavelength of the wrinkles (λ) is given by $2\pi/q_0$. The wavelength (open circles) is used to determine the Young's modulus of the film by means of eq 6.

length to elastic modulus is now well-established for a wide variety of thin film systems.^{30–35} This approach requires the transfer of the thin film of interest from a rigid substrate (e.g., silicon wafer, mica) to a soft elastic substrate (e.g., PDMS). Films that cannot be easily transferred may require additional strategies, such as release layers,^{34,35} but the applicability of surface wrinkling to measure material properties is still valid.

Here, we extend our previously reported wrinkling-based metrology³⁰ to arrive at the critical strain needed to produce surface wrinkling. For high precision, we use small-angle light scattering (SALS)³⁷ to measure the critical strain for onset of wrinkling. We find that the observed critical strain significantly differs from the theoretically predicted value. We use this difference, along with the wrinkling wavelength, to quantify residual strain and elastic modulus, thereby determining residual stress in polymer thin films. We compare our results with those obtained from the conventional wafer curvature-based technique and show that this wrinkling method is more accurate in determining the residual stress for thin (sub-1 μm) polystyrene films. To further demonstrate the utility of this new metrology, we use it to evaluate strategies commonly employed to dissipate residual stress in thin polymer films. First, we examine the impact of annealing the polymer above its glass transition temperature. Then, we examine the effect of added plasticizer and the relationships to changes in the glass transition on residual stress.

RESULTS AND DISCUSSION

Residual Stress Measurements via Surface Wrinkling. Our model system consists of a thin (sub-1 μm) glassy polystyrene (PS) film supported on a soft elastic substrate of poly(dimethylsiloxane) (PDMS). This PS/PDMS laminate is prepared by transferring a spin-cast PS film from a rigid substrate (e.g., silicon wafer, mica) to the softer PDMS substrate.³⁰ When a small uniaxial compressive strain is applied to this lami-

nate, wrinkling occurs above the critical strain with a well-ordered sinusoidal pattern that forms perpendicular to the compression direction. We measure the critical strain for the onset of wrinkling (ε_c) by monitoring the evolution of the scattered light intensity with increasing compressive strain using a custom-built SALS instrument (Figure 1a).

Figure 1b shows representative results for the evolution of the scattered intensity (I) and wrinkling wavelength (λ) for a PS film ($h_f \approx 100$ nm) on PDMS as a function of compressive strain (ε). For $\varepsilon < \varepsilon_c$, only a baseline intensity is observed since this strain is below the critical value for onset of wrinkling. When $\varepsilon > \varepsilon_c$, there is an abrupt transition between the nonwrinkled and wrinkled state, where the first-order diffraction intensity increases with strain due to the increasing wrinkling amplitude.^{26–28,37} Following the argument by Harrison *et al.*³⁷ along with the Fraunhofer approximation³⁸ and eq 2, the first-order diffraction intensity, $I(\varepsilon)$, can be expressed as

$$I(\varepsilon) = J_1^2 \left[\frac{2\pi(n-1)}{d} h_f \left(\frac{\varepsilon}{\varepsilon_c} - 1 \right)^{1/2} \right] \quad (4)$$

where d is the laser wavelength (633 nm), n is the index of refraction of PDMS (1.404 ± 0.004),³⁷ and $J_1(x)$ is the Bessel function of the first kind. For $0 < x \ll \sqrt{2}$ (using the typical experimental values of h_f , ε_c , and ε as 100 nm, 0.01, and < 0.02 , respectively, we find that $x < 0.4$), $J_1(x)$ becomes asymptotic and can be approximated as $J_1(x) \rightarrow x/2$. In this limit, eq 4 can be simplified as

$$I(\varepsilon) = \left(\frac{\pi(n-1)h_f}{d} \right)^2 \left(\frac{\varepsilon}{\varepsilon_c} - 1 \right) \quad (5)$$

where $I(\varepsilon)$ scales linearly with the applied strain. We use eqs 4 and 5 to predict the intensity data, and the results are shown in Figure 1b. Near the critical strain ($\varepsilon < 0.015$), the simplified expression (eq 5) can accurately predict the scattered intensity. While the full form (eq 4) is necessary to predict the intensity values for large strains, we can simply use eq 5 to predict the critical strain since it is possible to make a limited number of intensity measurements and extrapolate to the baseline intensity.

The observed critical strain (ε_c) was taken as the intersection of the two straight lines fitted *via* linear regression (Figure 1b) and was found to be $\varepsilon_c = 0.0114 \pm 0.0002$ in this example. We emphasize that the low level of uncertainty (relative standard deviation $< 0.2\%$) is representative of these measurements. Additionally, we can also simultaneously measure the elastic modulus (E_f) of the deposited film from the wrinkle wavelength (λ) by using eq 1:

$$E_f = \frac{3E_s(1-\nu_f^2)}{(1-\nu_s^2)} \left(\frac{\lambda}{2\pi h_f} \right)^3 \quad (6)$$

We point out here that, although the above equation (or eq 1) does not predict λ dependence on the applied strain, Rogers and co-workers have recently shown that λ changes with applied strain in an approximately linear manner.³⁹ Their findings may explain a slight decrease in λ over the range of strain that we examined (Figure 1b). Here, we confined our measurements to a small strain range (e.g., $\varepsilon < 0.015$), where λ is calculated to change by less than 2%.³⁹ Therefore, we treat λ as constant and use the average wrinkling wavelength (measured at $\varepsilon_c < \varepsilon < 0.015$) to determine the elastic modulus. In its current form, this measurement may not accurately describe samples subjected to large strains because of nonlinear elastic response or large deformation.⁴⁰

Using eq 6, the PS film modulus was determined to be $E_f = 3.69 \pm 0.04$ GPa using the average values of λ between $\varepsilon_c < \varepsilon < 0.015$. This modulus—along with $\nu_s = 0.50$, $\nu_f = 0.33$,⁴¹ and $E_s = 1.8$ MPa (see Materials and Methods)—was used to calculate the theoretical critical strain (ε_{c0}) *via* eq 3. The resulting theoretical critical strain was found to be $\varepsilon_{c0} = 0.0036$, which is more than three times lower than the observed critical strain ($\varepsilon_c = 0.0114$).

To explain this discrepancy, we first note that it is known that spin-coated polymer films possess measurable levels of residual stress. The magnitude of residual stress is related to the proximity of their glass transition temperature (T_g) to ambient conditions, as discussed in detail by Croll⁴ and by Reiter and de Gennes.⁶ In general, the mobility of polymer chains above T_g is enhanced, which allows the chains to relax and relieve their stress. Conversely, chain mobility is suppressed below T_g , which arrests relaxation processes. During the spin-coating process, a volatile solvent rapidly evaporates from the polymer film. Therefore, the polymer film vitrifies and shrinks when the apparent T_g of the concentrating solution reaches ambient temperature. As solidification proceeds, tensile residual stress is generated in the plane of the coating due to the large volume change coupled with the confining effect of the substrate, as suggested by several experimental observations and theoretical studies.^{2–6} If this tensile stress is not accounted for in our wrinkling experiments, it will lead to an “underestimate” of the critical strain since a higher compressive strain (or stress) will be required to induce wrinkling in the presence of tensile residual stress compared to the residual stress-free state (*i.e.*, reference state). This underestimate of the critical strain is consistent with observed and theoretical values associated with Figure 1b.

We postulate that the discrepancy between the observed and theoretical critical strain is predominantly attributed to the presence of residual strain, or residual stress, resulting from spin-casting process. To account for this residual strain, we assume that the observed critical strain (ε_c) is a sum of the theoretical critical strain (ε_{c0}) and the residual strain (ε_R):

$$\varepsilon_c = \frac{1}{4} \left(\frac{3\bar{E}_s}{\bar{E}_f} \right)^{2/3} + \varepsilon_R \quad (7a)$$

We note that the relationship between residual strain ($\varepsilon_R = \varepsilon_c - \varepsilon_{c0}$) and residual stress (σ_R) is given by

$$\sigma_R = \bar{E}_f \varepsilon_R \quad (7b)$$

On the basis of this relationship, the residual stress in the film was estimated to be $\sigma_R = 32.2$ MPa (here $\varepsilon_R = 0.0078$ and $\bar{E}_f = 4.14$ GPa). We note that our residual stress measurements do not require knowledge of the Poisson's ratio of the film (ν_f) because all of the calculations involved (eqs 6 and 7) are expressed in terms of plane-strain modulus of the film, $\bar{E}_f = E_f/(1 - \nu_f^2)$, which can be directly measured from the wrinkling wavelength without any prior assumption of the value of ν_f [$\bar{E}_f = 3\bar{E}_s(\lambda/2\pi h_f)^3$; modified from eq 6]. Thus, the uncertainty in the value of ν_f does not impact the stress value. To validate this approach for quantifying residual stress in thin polymer films, several evaluations of this wrinkling metrology were made. These include comparison with a conventional instrumental method, thermal annealing, and plasticization. As we present below, all of the observations support the hypothesis that the difference in observed and theoretical critical strain is primarily caused by the presence of residual stress in the polymer films examined in this study.

Comparison with a Conventional Measurement. We compare the residual stress values obtained from our wrinkling method to the commonly used wafer curvature-based approach. As shown in Figure 2a, the results obtained from our wrinkling method show that both the observed and theoretical critical strains are independent of the film thickness range explored (100–400 nm). This thickness independence also holds true for the PS film modulus and is approximately constant ($E_f = 3.71 \pm 0.25$ GPa; see inset Figure 2a), in agreement with previous results.³⁰ Hence, the residual stresses, calculated from eq 7, are approximately independent of the film thickness, with an average value of $\sigma_R = 31.9 \pm 4.7$ MPa. A positive residual stress value is considered tensile since the observed strain is greater than the theoretical strain (*i.e.*, a larger compressive strain is required to induce wrinkling), which was also confirmed by the curvature-based method (see below). This is expected since the residual strain (or stress) is caused by the shrinkage associated with solidification in solvent casting.^{2,4}

The residual stress results measured by the wafer curvature-based method (see Materials and Methods) for three different thicknesses of PS films ($h_f = 80, 160, 730$ nm) are shown in Figure 3. The main observation in Figure 3 is that the average magnitudes of residual stress (on the order of 10 MPa) are similar to those obtained by the surface wrinkling method. For example, for the results for a 200 nm film, the curvature method measured a residual stress of 30.4 MPa, whereas the wrinkling technique obtained a value of 29.0 MPa. This close agreement indicates that the stress level quantified by surface wrinkling corresponds predominantly to residual stress in the film.

More importantly, the uncertainty level of the curvature-based method becomes increasingly larger as film thickness decreases. This point is illustrated in the standard deviations for each set of curvature-based measurements, which represent the uncertainty in measuring residual stress. This large uncertainty is caused by the limited sensitivity of the instrument, which limits its resolution of the residual stress for thin films, particularly for the 80 nm thick PS film. For example, a detectable minimum curvature of 120 μm (radius ≈ 8000 m) corresponds to a minimum detectable stress of 1.3 MPa for a 588 μm thick Si wafer (100 mm in diameter) with a 1 μm thick film on it. For polymer films with thicknesses of 730, 160, and 80 nm, the corresponding minimum detectable stress will be 1.8, 8.1, and 16.2 MPa, respectively. As shown in Figure 3, the wrinkling method shows a much higher sensitivity in measuring residual stress even in thin films.

Effects of Thermal Annealing. Thermal annealing is known to relieve the residual stress in polymer systems (for example, see ref 1). To quantify the effects of thermal annealing on residual stress, we employ the wrinkling-based method to measure the residual stress in thermally annealed spin-cast PS films. Briefly, PS films were spin-cast from toluene onto mica substrates. They were then annealed for a controlled period of time at 155 $^{\circ}\text{C}$, well

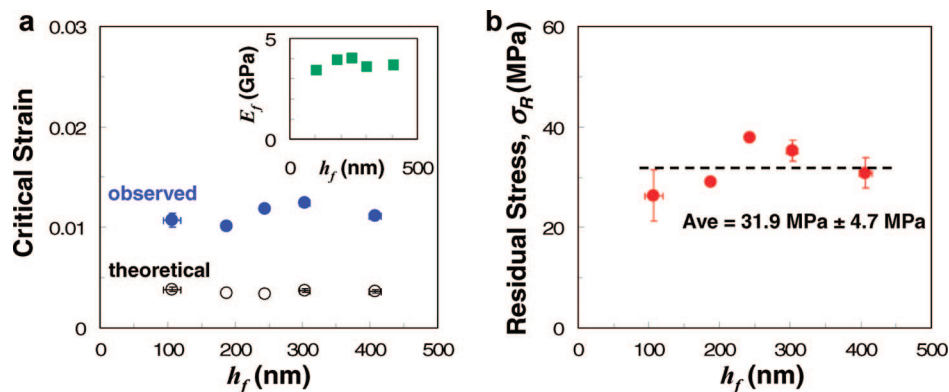


Figure 2. (a) Observed critical strain (closed circles) and theoretical critical strain (open circles) obtained as a function of film thickness (h_f). The inset displays the measured modulus as a function of h_f , which was calculated by means of eq 6 with the measured wavelength. (b) Corresponding residual stresses (σ_R) as a function of h_f . The dashed line is meant to guide the eye, and the error bars represent one standard deviation of the data, which is taken as the experimental uncertainty of the measurement.

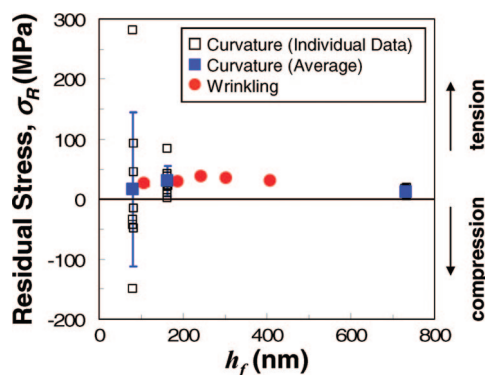


Figure 3. Residual stresses (σ_R) as a function of film thickness (h_f) measured by the wafer curvature-based technique. Open squares represent a single measurement. Closed squares are the average values obtained from at least eight individual measurements with the same thickness, and the error bars indicate the relative standard uncertainty of the measurement. Closed circles represent the residual stresses measured by the wrinkling method, which were reproduced from Figure 2b for comparison.

above the glass transition temperature of PS ($T_g = 105$ °C). After slow cooling (about 0.3 °C min^{-1}) to room temperature, the films were transferred onto PDMS and wrinkled. We note that, in these experiments, we used atomically flat mica substrates instead of silicon substrates because they facilitate film transfer after prolonged thermal annealing. No significant differences in σ_R values were observed for the unannealed PS films ($h_f \approx 100$ nm) cast onto either silicon (26.4 ± 5.1 MPa; Figure 2) or mica (27.6 ± 4.9 MPa; Figure 4) substrates.

Figure 4a shows the ε_c and ε_{c0} values for PS films ($h_f \approx 120$ nm) at room temperature obtained after annealing times up to 168 h. Since the room temperature modulus is constant, ε_{c0} remains constant. However, ε_c decays with increasing annealing time. The corresponding σ_{Rv} de-

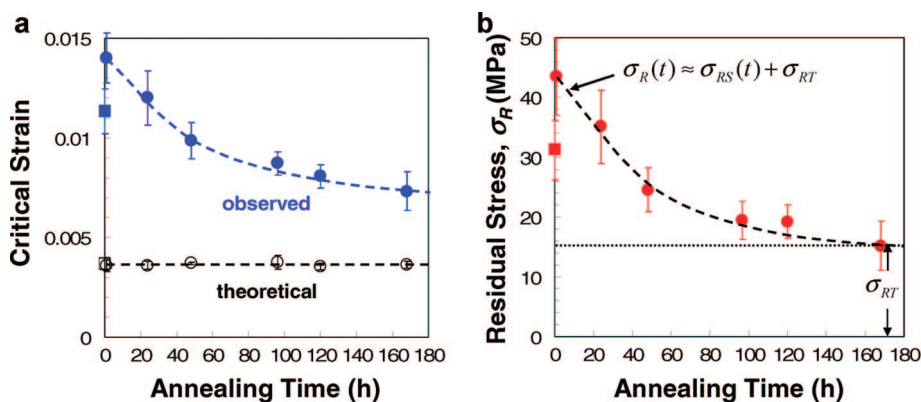


Figure 4. (a) Observed critical strain (ε_c) and theoretical critical strain (ε_{c0}) in PS films spin-coated onto mica substrates as a function of the annealing time ranging from 1 to 168 h. In all experiments, the film thickness was kept at $h_f \approx 120$ nm. The values of ε_c were determined directly from SALS intensity data, whereas ε_{c0} was indirectly calculated from the measured wrinkling wavelength with eqs 3 and 6. (b) Corresponding residual stresses (σ_R) as a function of annealing time. The measured residual stress at a given annealing time, $\sigma_R(t)$, can be decoupled into two terms: stress induced by spin coating, $\sigma_{RS}(t)$, which decreases and asymptotically approaches 0 as the annealing time increases, and a constant thermal stress, σ_{RT} , associated with cooling the sample to room temperature after annealing. In both plots, the square symbols represent the critical strain and residual stress in PS films spin-coated onto mica substrates without annealing. Dashed lines are added to guide the eye.

termined using eq 7, is shown in Figure 4b. The results suggest that thermal annealing leads to a decrease in the residual stress, and the apparent relaxation time ($\tau \approx 50$ h; see ref 42) observed in these spin-coated PS films seems to be quite long. This slow relaxation mode for spin-cast PS films seems similar to that observed by Kanaya *et al.*⁴³ and warrants further study.

Another interesting observation in Figure 4 is that the observed critical strain (and residual stress) measured at a relatively short annealing time ($t = 1$ h) is higher than values measured prior to thermal annealing (square symbols). Furthermore, the residual stress does not vanish even after long annealing times (e.g., 168 h). Instead, it reduces to a finite level (i.e., ε_{c0} and ε_c do not converge). This is because the residual stress arises from two sources: (1) the original level of residual stress imparted by spin coating (σ_{RS}) and (2) the stress inherent to thermal annealing (σ_{RT}) that arises upon cooling below T_g , due to the mismatch in coefficients of thermal expansion between the film and substrate. While the original residual stress caused by spin coating can be eliminated through thermal annealing above T_g , a “thermal stress” is inevitably produced upon cooling the sample after annealing, and this contribution to residual stress remains in the film.

The thermal stress (σ_{RT}) caused by mismatch of coefficients of thermal expansion (CTE) between the film and the substrate can be estimated as⁴⁴

$$\sigma_{RT} \cong \frac{E_f}{(1 - \nu_f^2)} (\alpha_f - \alpha_s) (T_{RT} - T_g) \quad (8)$$

where α is the coefficient of thermal expansion and T_{RT}

is room temperature (subscripts f and s denote the PS film and mica substrate, respectively). Using eq 8, we calculated $\sigma_{RT} \approx 16.6$ MPa using the following values: $E_f = 3.7$ GPa, $\nu_f = 0.33$, $\alpha_f \approx 60 \times 10^{-6}$ °C⁻¹ at $T < T_g$,^{11,45} $\alpha_s \approx 10 \times 10^{-6}$ °C⁻¹,⁴⁶ and $T_g = 105$ °C. This calculated thermal stress is in close agreement with the value (15.2 ± 4.1 MPa) obtained from our data at $t = 168$ h (Figure 4b). Accordingly, our data suggest that the measured residual stress at a given annealing time, $\sigma_R(t)$, can be viewed as a combination of the stress induced by spin coating, $\sigma_{RS}(t)$, which decreases with time by the thermal annealing process, and a constant thermal stress, σ_{RT} , induced upon cooling:

$$\sigma_R(t) = \sigma_{RS}(t) + \sigma_{RT} \quad (9)$$

To illustrate this point, the measured residual stress at short annealing time ($\sigma_R \approx 43.5$ MPa at $t = 1$ h) is approximately equivalent to the sum of stresses outlined in eq 9 ($27.6 + 15.2$ MPa = 42.8 MPa; see Figure 4b), where $\sigma_{RS} = 27.6$ MPa is taken as the stress in the unannealed film that was initially spin-cast on the mica substrate. With these results, it is evident that thermal annealing can significantly reduce or even eliminate the residual stress due to film formation in spin-cast thin polymer films. Our measurement method can accurately evaluate this type of phenomenon and demonstrates that thermal stress can be quantitatively related to the CTE differences, which allows this phenomenon to be decoupled from the original residual stress.

Effects of Plasticizer Addition. Plasticizers increase the mobility of polymer chains, which can be partially explained in terms of lowering the polymers' T_g in relation to the operating temperature. Hence, with enhanced mobility imparted by the plasticizer, it is expected that the residual stress can be relieved and reduced. To gauge the effects of plasticizer addition on the residual stress in spin-cast films, we prepared a model system comprising blends of PS with a nonvolatile plasticizer (dioctyl phthalate, DOP). Mixtures having different mass fractions of DOP (10–40%) were co-dissolved in toluene and then spin-coated onto silicon wafers. The films were then transferred onto PDMS and wrinkled. As presented in Figure 5a, the measured modulus (closed squares) of the PS film ($h_f \approx 200$ nm) decreases in a sigmoidal manner with increasing concentration of added plasticizer, following the trend previously observed.^{30,47} In addition, the theoretical critical strain (open circles) increases with increasing plasticizer concentration because the wrinkling inferred modulus (E_i) of the film decreases in a nonlinear way (see eq 3), and the observed critical strain (closed circles) decreases slightly as a function of plasticizer content. Thus, the residual strain decreases as the plasticizer concentration increases. As a

consequence of a decrease in both modulus and residual strain, we see a more pronounced decrease in residual stress (σ_R) with increased plasticizer concentration (Figure 5b).

It is well-known that the addition of DOP to PS leads to a significant reduction in T_g , accompanied by a decrease in modulus. In particular, the T_g of the mixture drops to roughly 20 °C for a plasticizer mass fraction of 30% (PS/DOP30) and 0 °C for a plasticizer mass fraction of 40% (PS/DOP40).⁴⁸ PS/DOP30 and PS/DOP40 at room temperature are above their T_g , and the residual stress diminishes to a negligible level or 0, which is particularly striking when compared with the nonplasticized PS film ($\sigma_R \approx 30$ MPa). Overall, the results imply that the decrease in σ_R with increasing plasticizer content is attributed to the lower E_f in addition to the lower levels of constrained shrinkage due to the lower T_g . We note that the same conclusion was deduced by Francis *et al.*² in their comprehensive review.

Residual Stresses in Ultrathin Polymer Films. A significant advantage in our wrinkling approach is that it can accurately quantify residual stress in ultrathin (<100 nm) polymer films. For PS films with thicknesses ranging from 24 to 100 nm, their modulus (closed squares) exhibits a significant decrease with decreasing film thickness (Figure 6a), which corroborates previous results.⁴⁹ In addition, as the film thickness decreases, ε_{c0} increases and ε_c decreases slightly. As shown in Figure 6b, the measured residual stresses drop considerably for the two thinnest films studied (24 and 30 nm), with the residual stresses found to be 5.5 and 8.9 MPa, respectively. This is nearly an order of magnitude smaller than those obtained for the PS films with thickness above 100 nm ($\sigma_R \approx 30$ MPa; see Figure 2b). These results highlight the potential to quantitatively describe important phenomena in ultrathin films. For example, it has been reported that the T_g of ultrathin films can differ from the bulk.^{50–55} Our findings of a decrease in residual stress may correlate with a decrease in T_g . In addition, it has been shown that spin-cast ultrathin PS films retain

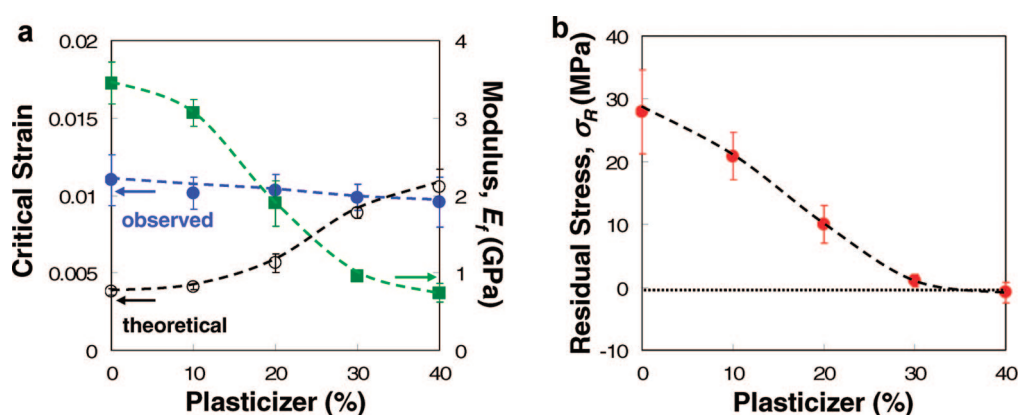


Figure 5. (a) Observed critical strain (closed circles) and theoretical critical strain (open circles) obtained as a function of plasticizer (DOP) mass fraction. Closed squares show the measured modulus, which is calculated by means of eq 6 with the measured wavelength. (b) Corresponding residual stress as a function of plasticizer mass fraction. In both plots, the dashed lines are meant to guide the eye.

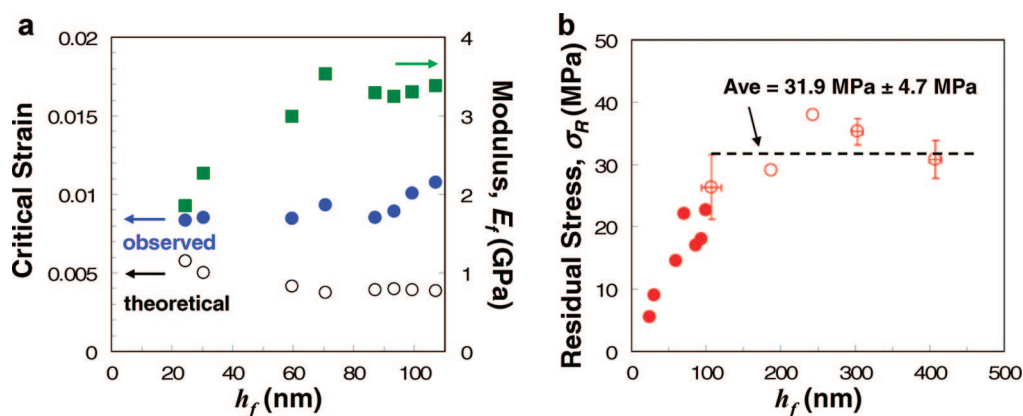


Figure 6. (a) Observed critical strain by SALS (closed circles) and theoretical critical strain (open circles) obtained as a function of film thickness (h_f). The closed squares represent the measured moduli at different h_f , which were calculated by means of eq 6 with the measured wavelengths. (b) Corresponding residual stresses (σ_R ; closed circles) as a function of h_f . Note that the data above $h_f \approx 100$ nm (open circles) were reproduced from Figure 2b for comparison. The dashed line is meant to guide the eye, representing the average residual stress above $h_f \approx 100$ nm. In both plots, each data point represents a single measurement; however, the uncertainty in measuring critical strain is small (relative standard deviation $<0.2\%$).

higher levels of residual toluene,^{7,56} which could lower the residual stress similarly to the effect of added plasticizers. Our results do not fully probe these important aspects of ultrathin films. Nevertheless, this capability to quantitatively probe the residual stress in ultrathin films should ultimately provide important new insight.

CONCLUSION

We have presented a new method for determining residual stress in polymer thin films using strain-induced wrinkling. We have examined residual stresses of spin-cast PS films with thickness in the nanometer-scale range (20–400 nm). This method relies on detecting the critical strain needed to produce surface wrinkling and the wrinkling wavelength, both of which can be easily and accurately measured, even in ultrathin films. Our wrinkling metrology found equivalent levels of residual stress in equivalent spin-cast PS films when compared with a conventional curvature-based

method. The wrinkling method, however, exhibited higher sensitivity and more accurate measurement of residual stress in much thinner films and softer systems. Our approach further provided qualitative insight into two widely used strategies for the dissipation of residual stress in polymer thin films, including thermal annealing and plasticizer addition. It is expected that further application of this method will allow for new insight into details of residual stress. It is also noted that considerations of residual stress, to a large extent, have not been incorporated into the theoretical framework associated with polymer thin films, and this is due in part to limited measurement methods to quantify this phenomenon experimentally. Our robust and simple route to measure residual stress addresses this limitation and should provide a better understanding that will enable identification of more effective processing routes that mitigate the detrimental effects of residual stress.

MATERIALS AND METHODS

General. Certain commercial materials and equipment are identified in this paper in order to specify adequately the experimental procedure. In no case does such identification imply recommendation by the National Institute of Standards and Technology nor does it imply that the material or equipment identified is necessarily the best available for this purpose. The error bars presented throughout this paper indicate one standard deviation of the data, which is taken as the experimental uncertainty of the measurement.

Materials and Sample Preparation. We used an atactic PS (Polymer Source, Inc.): $M_w = 654.4 \times 10^3$ g mol⁻¹, $M_w/M_n = 1.09$, where M_w is the mass-average and M_n is the number-average molecular mass. Thin PS films of various thickness were prepared by spin-casting from dilute toluene (anhydrous, 99.8%, Sigma-Aldrich) solutions onto polished silicon (100) wafers (Silicon Quest International, Inc.), which had been pretreated by ultraviolet-ozone cleaner (5 min; Model 342, Jelight) to make the surface hydrophilic. All solutions were filtered through a 0.45 μ m Acrodisc filter prior to spin-coating. The film thickness was controlled by varying the polymer concentration in solution (0.25–5.0% by mass polymer) while maintaining the same spin-

coating conditions. All the samples tested in this work were dried for about 1 h under ambient conditions prior to measurements. We note that previous reports have found that some residual toluene remains in spin-cast PS films—for most PS films (>100 nm), only a few percent of toluene by mass remained, although ultrathin PS films (<100 nm) were found to contain increasing amounts of toluene.^{7,56} The thickness of each film was measured by a reflectance interferometry (minimum nine measurements per sample; Model F20, Filmetrics).

For the annealing experiments, thin PS films were prepared by spin-casting from dilute toluene solutions onto freshly cleaved mica substrates (Grade V2, Ted Pella, Inc.). These samples were annealed in a vacuum oven at 155 $^{\circ}$ C, well above the T_g of PS (105 $^{\circ}$ C), for times ranging from 1 to 168 h, and then slowly cooled to room temperature at a rate of approximately 0.3 $^{\circ}$ C min⁻¹.

Binary mixtures of PS with a common plasticizer (dioctyl phthalate, DOP) were prepared with varying amounts of the plasticizer mass fraction (10–40%). The mixtures were co-dissolved in toluene and deposited onto silicon wafers by spin-casting.

PDMS elastomer (Sylgard 184, Dow Chemical Co.) was prepared by hand-mixing an oligomeric base and a curing agent

(10:1 by mass), which was cast onto glass plates. The mixture was left at room temperature overnight to allow trapped air bubbles to escape and then cured at 75 °C for 2 h. After curing, the PDMS sheet (thickness \approx 2.5 mm) was cut into 75 mm \times 25 mm specimens. The modulus of the PDMS was $E_s = 1.8 \pm 0.1$ MPa as measured before each experiment by tensile tests (Texture Analyzer, Model TA.XT2i, Texture Technologies). In all experiments presented here, the Poisson's ratios of PDMS substrates and PS films were chosen to be 0.50 and 0.33,⁴¹ respectively.

To prepare samples for testing, spin-cast polymer films were transferred from substrates (e.g., silicon wafer, mica) to the surface of PDMS substrates as described previously.^{30,37} Specifically, a centimeter-sized square was cleaved from the spin-coated substrate and placed film-side down onto a prestretched slab of PDMS mounted on a computer-controlled strain stage. The PDMS/film/substrate laminate was immersed under water. Water wets the interface between the hydrophilic wafer (or mica) and the polymer film, thereby transferring the film from the substrate onto the PDMS with little or no stress being applied to the film. The tackiness of the PDMS assures very good adhesion of the PS film. We note that the PS films were not allowed to be in the free state at any time. Samples were allowed to dry under ambient conditions for about 1 h prior to wrinkling measurements.

Wrinkling-Based Measurements. After the film had been transferred to the PDMS surface, a uniaxial compressive strain was applied to the specimen at a constant rate using the translation stage in order to induce wrinkling. The critical strain for the onset of wrinkling was determined by observing the intensity of scattered light on a custom-built small-angle light scattering (SALS) instrument (Figure 1a), following a procedure similar to that previously described.^{30,37} SALS was performed on samples in transmission mode with a low-power red (633 nm) helium–neon laser (beam diameter = 0.52 mm; Melles Griot) and a charge-coupled-device (CCD) camera (RTE/CCD-1300-V/HS, Roper Scientific Inc.). As coherent light passes through a wrinkled surface, a local phase shift is imparted with a magnitude proportional to the wrinkling amplitude. In our initial experiments, we systematically varied the velocity of the translation stage from 2 to 100 $\mu\text{m s}^{-1}$. The observed values of critical strain were constant (within error bars) over this velocity range, illustrating the elastic behavior of polymers. In all experiments presented here, the velocity of the translation stage was fixed at 10 $\mu\text{m s}^{-1}$. We also note that, throughout this paper, “strain” refers to the degree of compression of the polymer film, not the prestretched PDMS.

Curvature-Based Measurements. A laser reflection-based surface curvature and stress measurement system (KLA-Tencor Flexus System, Model FLX-2320, Toho Technology) was used to measure the residual stress of the PS films by measuring the initial (R_0) and final radius of curvature (R) of a substrate before and after film deposition as^{18,19}

$$\sigma_R = \frac{E_s h_s^2}{6(1 - \nu_s) h_f} \left(\frac{1}{R} - \frac{1}{R_0} \right) \quad (10)$$

The curvature of each wafer was analyzed at every 45° at room temperature followed by deposition of PS films by spin-coating. The curvature of the PS films on the pre-examined wafer was measured with the same method. The PS films having the same properties as those of the wrinkling measurements were prepared with three different thicknesses (80, 160, 730 nm), and the curvature measurements were repeated three times. For all the samples, the same spin-coating condition (1200 rpm for 60 s) was used. The thicknesses of the polymer films and the Si wafers were measured by a reflectance interferometry (Model F20, Filmetrics) and by a Digimatic Indicator (Mitutoyo Corp.), respectively. Si (100) wafers (100 mm in diameter) with the thickness of $h_s = 588(\pm 2)$ μm and the biaxial modulus of $E_s/(1 - \nu_s) = 180$ GPa were used to calculate for the residual stress.

Acknowledgment. We acknowledge the Nanofabrication Laboratory of the NIST Center for Nanoscale Science and Technology (CNST) for providing the FLX-2320 film stress measurement tool, and Gerard E. Henein for measurement assistance. We thank Rui Huang for insightful discussions regarding the wrin-

gling mechanics models, and Edwin P. Chan for careful reading of the manuscript. T.Q.C. recognizes the support of the NIST/NRC Postdoctoral Fellowship Program.

REFERENCES AND NOTES

- Frank, C. W.; Rao, V.; Despotopoulou, M. M.; Pease, R. F. W.; Hinsberg, W. D.; Miller, R. D.; Rabolt, J. F. Structure in Thin and Ultrathin Spin-Cast Polymer Films. *Science* **1996**, *273*, 912–915.
- Francis, L. F.; McCormick, A. V.; Vaessen, D. M.; Payne, J. A. Development and Measurement of Stress in Polymer Coatings. *J. Mater. Sci.* **2002**, *37*, 4897–4911.
- Croll, S. G. Internal-Stress in a Solvent-Cast Thermoplastic Coating. *J. Coat. Technol.* **1978**, *50*, 33–38.
- Croll, S. G. Origin of Residual Internal-Stress in Solvent-Cast Thermoplastic Coatings. *J. Appl. Polym. Sci.* **1979**, *23*, 847–858.
- Ree, M.; Swanson, S.; Volksen, W. Effect of Precursor History on Residual-Stress and Relaxation Behavior of High-Temperature Polyimides. *Polymer* **1993**, *34*, 1423–1430.
- Reiter, G.; de Gennes, P. G. Spin-Cast, Thin, Glassy Polymer Films: Highly Metastable Forms of Matter. *Eur. Phys. J. E* **2001**, *6*, 25–28.
- Richardson, H.; Carelli, C.; Keddie, J. L.; Sferazza, M. Structural Relaxation of Spin-Cast Glassy Polymer Thin Films As a Possible Factor in Dewetting. *Eur. Phys. J. E* **2003**, *12*, 437–440.
- Reiter, G.; Hamieh, M.; Damman, P.; Sclavons, S.; Gabriele, S.; Vilmin, T.; Raphael, E. Residual Stresses in Thin Polymer Films Cause Rupture and Dominate Early Stages of Dewetting. *Nat. Mater.* **2005**, *4*, 754–758.
- Damman, P.; Gabriele, S.; Coppee, S.; Desprez, S.; Villers, D.; Vilmin, T.; Raphael, E.; Hamieh, M.; Al Akhrass, S.; Reiter, G. Relaxation of Residual Stress and Reentanglement of Polymers in Spin-Coated Films. *Phys. Rev. Lett.* **2007**, *99*, 036101.
- Akhrass, S. A.; Reiter, G.; Hou, S. Y.; Yang, M. H.; Chang, Y. L.; Chang, F. C.; Wang, C. F.; Yang, A. C. M. Vicoelastic Thin Polymer Films under Transient Residual Stresses: Two-Stage Dewetting on Soft Substrates. *Phys. Rev. Lett.* **2008**, *100*, 178301.
- Zhao, J. H.; Kiene, M.; Hu, C.; Ho, P. S. Thermal Stress and Glass Transition of Ultrathin Polystyrene Films. *Appl. Phys. Lett.* **2000**, *77*, 2843–2845.
- Perera, D. Y.; Vanden Eynde, D. Considerations on a Cantilever (Beam) Method for Measuring the Internal-Stress in Organic Coatings. *J. Coat. Technol.* **1981**, *53*, 39–44.
- Xu, Y. H.; Tsai, Y.; Zheng, D. W.; Tu, K. N.; Ong, C. W.; Choy, C. L.; Zhao, B.; Liu, Q.-Z.; Brongo, M. Measurement of Mechanical Properties for Dense and Porous Polymer Films Having a Low Dielectric Constant. *J. Appl. Phys.* **2000**, *88*, 5744–5750.
- Guo, S.; Wan, K.-T.; Dillard, D. A. A Bending-to-Stretching Analysis of the Blister Test in the Presence of Tensile Residual Stress. *Int. J. Solid Struct.* **2005**, *42*, 2771–2784.
- Ju, B.-F.; Liu, K.-K.; Wong, M.-F.; Wan, K.-T. A Novel Cylindrical Punch Method to Characterize Interfacial Adhesion and Residual Stress of a Thin Polymer Film. *Eng. Fract. Mech.* **2007**, *74*, 1101–1106.
- Shiga, T.; Narita, T.; Ikawa, T.; Okada, A. Stress Monitoring in Thin Polymer Coatings Using Time Resolved Fluorescence. *Polym. Eng. Sci.* **1998**, *38*, 693–698.
- Muraki, N.; Matoba, N.; Hirano, T.; Yoshikawa, M. Determination of Thermal Stress Distribution in a Model Microelectronic Device Encapsulated with Alumina Filled Epoxy Resin Using Fluorescence Spectroscopy. *Polymer* **2002**, *43*, 1277–1285.
- Stoney, G. G. The Tension of Metallic Films Deposited by Electrolysis. *Proc. R. Soc. London, Ser. A* **1909**, *82*, 172–175.
- Hoffman, R. W. In *Physics of Thin Films*; Hass, G., Thun, R. E., Eds.; Academic: New York, 1966; Vol. 3, p 211.
- Tang, Y. J.; Chen, J.; Huang, Y. B.; Li, D. C.; Wang, S. S.; Li, Z. H.; Zhang, W. D. Ultra-Sensitive, Highly Reproducible Film Stress Characterization Using Flexible Suspended

- Thin Silicon Plates and Local Curvature Measurements. *J. Micromech. Microeng.* **2007**, *17*, 1923–1930.
21. Bowden, N.; Brittain, S.; Evans, A. G.; Hutchinson, J. W.; Whitesides, G. M. Spontaneous Formation of Ordered Structures in Thin Films of Metals Supported on an Elastomeric Polymer. *Nature* **1998**, *393*, 146–149.
 22. Groenewold, J. Wrinkling of Plates Coupled with Soft Elastic Media. *Physica A* **2001**, *298*, 32–45.
 23. Allen, H. G. *Analysis and Design of Structural Sandwich Panels*; Pergamon Press: Oxford, 1969; Chapter 8.
 24. Volynskii, A. L.; Bazhenov, S.; Lebedeva, O. V.; Bakeev, N. F. Mechanical Buckling Instability of Thin Coatings Deposited on Soft Polymer Substrates. *J. Mater. Sci.* **2000**, *35*, 547–554.
 25. Huang, R. Kinetic Wrinkling of an Elastic Film on a Viscoelastic Substrate. *J. Mech. Phys. Solids* **2005**, *53*, 63–89.
 26. Chen, X.; Hutchinson, J. W. Herringbone Buckling Patterns of Compressed Thin Films on Compliant Substrates. *J. Appl. Mech.* **2004**, *71*, 597–603.
 27. Breid, D.; Crosby, A. J. Surface Wrinkling Behavior of Finite Circular Plates. *Soft Matter* **2009**, *5*, 425–431.
 28. Chung, J. Y.; Youngblood, J. P.; Stafford, C. M. Anisotropic Wetting on Tunable Micro-Wrinkled Surfaces. *Soft Matter* **2007**, *3*, 1163–1169.
 29. Mei, H. X.; Huang, R.; Chung, J. Y.; Stafford, C. M.; Yu, H. H. Buckling Modes of Elastic Thin Films on Elastic Substrates. *Appl. Phys. Lett.* **2007**, *90*, 151902.
 30. Stafford, C. M.; Harrison, C.; Beers, K. L.; Karim, A.; Amis, E. J.; Vanlandingham, M. R.; Kim, H.-C.; Volksen, W.; Miller, R. D.; Simonyi, E. E. A Buckling-Based Metrology for Measuring the Elastic Moduli of Polymeric Thin Films. *Nat. Mater.* **2004**, *3*, 545–550.
 31. Nolte, A. J.; Rubner, M. F.; Cohen, R. E. Determining the Young's Modulus of Polyelectrolyte Multilayer Films via Stress-Induced Mechanical Buckling Instabilities. *Macromolecules* **2005**, *38*, 5367–5370.
 32. Jiang, C.; Singamaneni, S.; Merrick, E.; Tsukruk, V. V. Complex Buckling Instability Patterns of Nanomembranes with Encapsulated Gold Nanoparticle Arrays. *Nano Lett.* **2006**, *6*, 2254–2259.
 33. Huang, H.; Chung, J. Y.; Nolte, A. J.; Stafford, C. M. Characterizing Polymer Brushes via Surface Wrinkling. *Chem. Mater.* **2007**, *19*, 6555–6560.
 34. Khang, D. Y.; Xiao, J. L.; Kocabas, C.; MacLaren, S.; Banks, T.; Jiang, H. Q.; Huang, Y. Y.; Rogers, J. A. Molecular Scale Buckling Mechanics on Individual Aligned Single-Wall Carbon Nanotubes on Elastomeric Substrates. *Nano Lett.* **2008**, *8*, 124–130.
 35. Aamer, K. A.; Stafford, C. M.; Richter, L. J.; Kohn, J.; Becker, M. L. Thin Film Elastic Modulus of Degradable Tyrosine-Derived Polycarbonate Biomaterials and Their Blends. *Macromolecules* **2009**, *42*, 1212–1218.
 36. We note that there is a slight discrepancy in the critical strain formulas developed by Volynskii *et al.*²⁴ (also Huang²⁵ and Chen and Hutchinson²⁶) and by Groenewold.²² Groenewold's formula, although having qualitatively the same form as eq 3, differs in magnitude by a factor of 2 ($\epsilon_{co} = (3\bar{E}_s/\bar{E})^{2/3}/2$); this equation was reformulated from eq 16 in ref 22 by taking $\nu_s = 1/2$. In this work, we have chosen to work with eq 3 since we believe that it is derived from a more comprehensive and rigorous analysis of the mechanics.
 37. Harrison, C.; Stafford, C. M.; Zhang, W. H.; Karim, A. Sinusoidal Phase Grating Created by a Tunably Buckled Surface. *Appl. Phys. Lett.* **2004**, *85*, 4016–4018.
 38. Goodman, J. W. *Introduction to Fourier Optics*, 2nd ed.; McGraw-Hill: New York, 1969.
 39. Jiang, H. Q.; Khang, D. Y.; Song, J. Z.; Sun, Y. G.; Huang, Y. G.; Rogers, J. A. Finite Deformation Mechanics in Buckled Thin Films on Compliant Supports. *Proc. Natl. Acad. Sci. U.S.A.* **2007**, *104*, 15607–15612.
 40. Lin, P.-C.; Yang, S. Spontaneous Formation of One-Dimensional Ripples in Transit to Highly Ordered Two-Dimensional Herringbone Structures Through Sequential and Unequal Biaxial Mechanical Stretching. *Appl. Phys. Lett.* **2007**, *90*, 241903.
 41. Brandrup, J.; Immergut, E. H., Eds. *Polymer Handbook*, 4th ed.; Wiley: New York, 1999; Section V, p 93. We note that it is unclear how Poisson's ratio varies with film thickness, especially in the ultrathin regime ($h_f < 100$ nm). In this work, we report values of the Young's modulus of the film (E_f) calculated with the assumption that bulk values of Poisson's ratio ($\nu_f = 0.33$) are valid for thin films. This topic is an important area for future study.
 42. We fitted the decay curve of σ_R (shown in Figure 4b) with a single exponential function as $\sigma_{RT}\exp[-(t/\tau)] + \sigma_{RT}$ to determine a relaxation time (τ). Here, σ_{RT} and σ_{RT} represent the initial residual stress ($t = 1$ h) and the residual stress for a sufficiently long time ($t = 168$ h), respectively. From the curve fitting with experimental data, τ was estimated to be approximately 50 h.
 43. Kanaya, T.; Miyazaki, T.; Watanabe, H.; Nishida, K.; Yamana, H.; Tasaki, S.; Bucknall, D. B. Annealing Effects on Thickness of Polystyrene Thin Films as Studied by Neutron Reflectivity. *Polymer* **2003**, *44*, 3769–3773.
 44. Film constraints impose plane-strain conditions, so we used plane-strain modulus $E_f/(1-\nu_f^2)$ in eq 8, rather than the biaxial modulus ($E_f/(1-\nu_f)$) used by Ho and co-workers¹¹ and by Hoffman.¹⁹
 45. Wallace, W. E.; van Zanten, J. H.; Wu, W. L. Influence of an Impenetrable Interface on a Polymer Glass-Transition Temperature. *Phys. Rev. E* **1995**, *52*, R3329–R3332.
 46. Hidnert, P.; Dickson, G. Some Physical Properties of Mica. *J. Res. Nat. Bur. Stand.* **1945**, *35*, 309–353.
 47. Huang, J.; Juszkiwicz, M.; de Jeu, W. H.; Cerda, E.; Emrick, T.; Menon, N.; Russell, T. P. Capillary Wrinkling of Floating Thin Polymer Films. *Science* **2007**, *317*, 650–653.
 48. Savin, D. A.; Larson, A. M.; Lodge, T. P. Effect of Composition on the Width of the Calorimetric Glass Transition in Polymer–Solvent and Solvent–Solvent Mixtures. *J. Polym. Sci., Part B* **2004**, *42*, 1155–1163.
 49. Stafford, C. M.; Vogt, B. D.; Harrison, C.; Jultongpipit, D.; Huang, R. Elastic Moduli of Ultrathin Amorphous Polymer Films. *Macromolecules* **2006**, *39*, 5095–5099.
 50. Keddie, J. L.; Jones, R. A. L.; Cory, R. A. Size-Dependent Depression of the Glass-Transition Temperature in Polymer-Films. *Europhys. Lett.* **1994**, *27*, 59–64.
 51. Forrest, J. A.; Dalnoki-Veress, K.; Stevens, J. R.; Dutcher, J. R. Effect of Free Surfaces on the Glass Transition Temperature of Thin Polymer Films. *Phys. Rev. Lett.* **1996**, *77*, 2002–2005.
 52. Fryer, D. S.; Nealey, P. F.; de Pablo, J. J. Thermal Probe Measurements of the Glass Transition Temperature for Ultrathin Polymer Films as a Function of Thickness. *Macromolecules* **2000**, *33*, 6439–6447.
 53. Forrest, J. A.; Dalnoki-Veress, K. The Glass Transition in Thin Polymer Films. *Adv. Colloid Interface Sci.* **2001**, *94*, 167–196.
 54. Ellison, C. J.; Torkelson, J. M. The Distribution of Glass-Transition Temperatures in Nanoscopically Confined Glass Formers. *Nat. Mater.* **2003**, *2*, 695–700.
 55. Alcoutlabi, M.; McKenna, G. B. Effects of Confinement on Material Behaviour at the Nanometre Size Scale. *J. Phys.: Condens. Matter* **2005**, *17*, R461–R524.
 56. García-Turiel, J.; Jérôme, B. Solvent Retention in Thin Polymer Films Studied by Gas Chromatography. *Colloid Polym. Sci.* **2007**, *285*, 1617–1623.